SLAC – PUB – 5040
August 1989
(N)

Design Considerations for a Čerenkov Ring Imaging Detector at the Tau-Charm Factory*

B. N. RATCLIFF

Stanford Linear Accelerator Center
Stanford University, Stanford, California 94309

ABSTRACT

A schematic design of a Čerenkov ring imaging detector for use at a τ-charm factory is described. The performance of this device and its implications for the other parts of the spectrometer are discussed.

Presented at the Tau-Charm Factory Workshop,
SLAC, Stanford, CA, May 23-27, 1989.

* Work supported by the Department of Energy under contract No. DE-AC03-76SF00515.

1. Introduction

It has been demonstrated at this workshop that a τ-charm factory detector needs very high-quality particle identification. The most difficult problems seem to be K/π separation above 900 MeV/c, e/π separation below 1 GeV/c, and μ/π separation in the region below about 600 MeV/c where separation in dense tracking chambers becomes difficult. As discussed elsewhere [1, 2], it may be possible to extend the "classical" techniques of time-of-flight and dE/dx to cover some of the difficult regions. Another approach, which is discussed here, is to use the ring imaging Čerenkov technology which promises superior particle identification performance [3]. A candidate device can be based on the Čerenkov Ring Imaging Detector (CRID) now being built for the SLD [4]. Although no large scale 4π acceptance devices are now in operation, two rather similar Čerenkov detectors are now under construction—the CRID for SLD and the RICH for DELPHI [5]; their performance in prototypes is well established [7, 8], and within about a year their operation in the colliding beam environment should be understood, so that it will soon be clear if the promise will be met in practice. A CRID is a rather complex device and contains a significant amount of material which unavoidably effects the performance of the electromagnetic calorimetry. A schematic design for a CRID, a discussion of its performance and mass, and a brief discussion of costs are presented. For this exercise, we will make use of existing techniques developed for the SLD to the maximum extent possible. Changes in some of these features may be desirable in a real device.

2. Principles of CRID Operation

As shown in Fig. 1, when a charged particle passes perpendicularly though a thin liquid radiator, it produces a cone of light whose angle depends on the particle velocity and the index of refraction of the liquid. If this Čerenkov light is allowed to propagate some distance before hitting the photon detector, it will form an image which is said to be "proximity focused" on the detector. For our geometry, using liquid C_6F_{14} with an index of refraction $n = 1.277$, the proximity focused circle for a relativistic ($\beta = 1$) particle is around 17 cm radius. There are typically around 25 photoelectrons produced for tracks which cross the liquid radiator at normal incidents, but some photons get lost by total internal reflection for angles exceeding $\sim 13°$, so that more typically there are around 14 photoelectrons observed.

The Čerenkov photons from the charged particle of interest pass through quartz windows in the liquid radiator cell and the detector box and are converted by photoionization of gaseous Tetrakis Dimethyl Amino Ethylene (TMAE), which has a very high quantum efficiency in the range 170 to 220 nm. The photoelectrons drift at constant velocity in a uniform electric field along the box until they arrive at a proportional wire detector. The position of the photoelectron conversion must be measured in three-space. Two coordinates come from the drift time of the electrons and the wire address of the hit wire, while charge division on the proportional wires determines the conversion depth in the box.

3. Geometry

Conceptually, a CRID would sit just outside the central tracker, in front of a TOF (if any) and the calorimeter as indicated in Fig. 2(a). The barrel CRID can start at any radius (or at any z distance for an end cap device) determined only by the outer dimensions of the tracker. However, the thickness of the device is essentially "fixed" at around 20 cm; that is, the performance of a thinner device will be compromised. An end cap can be re-entrant to make an approximately hermetic

device in theta. However, cracks between the liquid radiator boxes will lead to approximately 1–3% acceptance loss in azimuth. A cross section of the CRID is shown in Fig. 2(b). Starting from the inside, a particle first passes through an inner wall which in this design is a HEXCELL cylinder with aluminum skins. It then passes through the 4 mm-thick G-10 back of the liquid radiator tray, through 1 cm of C_6F_{14}, and out through the 4 mm-thick quartz window of the liquid radiator tray into a 13 cm drift region filled with a UV transmitting gas with good HV properties (such as a light fluorocarbon). It then passes through a 3 mm quartz window into the 4.4 cm photon conversion region of the drift box (containing C_2H_6 plus TMAE), through the 3 mm back wall of the drift box, and finally through about 7 mm of epoxy equivalent in a HV degrader of the ALEPH/DELPHI type [5, 6].

4. Technology

As will be shown, SLD technology with a liquid radiator matches the particle ID requirements for $\pi/K/p$ extremely well and also gives significant help to the calorimeters for low momentum e and μ identification. The device, as previously described, is essentially a liquid only version of the SLD CRID except:

1. there is an outer volume degrader, which is necessary to keep the space requirements down if a long drift configuration is chosen for the detector;
2. this CRID can be run at room temperature, which makes the gas and fluid systems much simpler with little effect on performance for a liquid radiator only system;
3. a fast read-out system is necessary to handle the 1 KHz trigger rates (see below).

5. Potential Problems of the Technology

The CRID uses a long drift ($\approx$ 25 μs), with the drift occurring over many beam crossings. Thus, there could be significant sensitivity to machine dependent backgrounds at the τ-charm factory, even though this does not appear to be a significant problem as far as these levels are presently understood. If in the future it becomes clear that such backgrounds are an important issue, then a different technology for photoelectron detection, such as the pad scheme discussed by Arnold et al., [9], would need to be seriously considered. However, it must be realized that a new readout scheme requires substantial R&D effort, which is now underway [9]. The pad schemes typically require a gaseous photocathode with short absorption length. The best developed of these proposals uses TEA as the photocathode, and thus requires a Čerenkov radiator which is transparent in the vacuum UV well below quartz cutoff. The suggested radiator (calcium fluoride) is a solid which has the virtue of eliminating the liquid handling problem. However, with an index of refraction above 1.5 in the TEA sensitive region, the resolution of the counter is compromised. More precisely, for a fixed figure of merit N_0, a fixed radiator length, and a fixed angular resolution on each Čerenkov photon, the resolution in β scales linearly with index of refraction n. Though the π/K separation of a solid radiator device should extend up to about 3 GeV and is completely adequate, the π/e and π/μ performance will be compromised. Moreover, the high index means that all the photons from fast particles near normal incidence get cut off by total internal reflection. A stepped radiator can alleviate this problem, but it will take space, will be more complicated, and some number of photons will always be lost.

The CRID contains approximately 20% of a radiation length of material distributed as follows:

1.	Inner wall	=	0.018 (L/L_{RAD})
2.	Liquid radiator tray	=	0.105 (L/L_{RAD})
3.	Drift box	=	0.044 (L/L_{RAD})
4.	Outer degrader wall	=	0.036 (L/L_{RAD})
5.	Total	=	0.203 (L/L_{RAD})

Significant reductions in this mass inventory are difficult, so that substantial effects on precision electromagnetic calorimetry seem unavoidable in any detector which contains a CRID of the SLD type. Moreover, the device has a "bad geometry" in that much of the mass is located a long way from the calorimeter. There are possibilities for modifications to the technology which could both reduce the total mass in the device and improve its distribution, but more generally, a CRID built for a general purpose detector probably needs to be removable so that some physics runs can be made with the detector in a low mass configuration in order to do the important physics that needs very low mass before the calorimeter. The space normally devoted to the CRID either be left unfilled or filled with another special purpose device of low mass.

A CRID is a rather expensive device to construct. In general, the component costs scale approximately with the area covered, whereas the electronic costs scale linearly with the radius. A fair estimate of the costs can be derived from actual SLD costs. If we assume a τ-charm detector similar to that described by Kirkby [10], which has a 60 cm radius by 250 cm long central drift chamber, the estimated costs are as follows:

Barrel (Total)		\$1245K
• Vessel	336K	
• Liquid Radiator (\$17K/m^2)	160K	
• Drift Box (\$40K/m^2)	377K	
• e^- Detectors (\$19K/m^2)	72K	
• ED&I	300K	
End Cap (Total)		558K
• Vessel	225K	
• Liquid Radiator (\$17K/m^2)	25K	
• Drift Box (\$40K/m^2)	60K	
• e^- Detectors (\$19K/m^2)	48K	
• ED&I	200K	
Fluid Control Monitor		500K
Electronics		1080K
CRID (Total)		\$3383K

6. Electronics

The SLD CRID electronics are matched to the properties of the SLC environment: for example, the trigger rate is slow (typically 1 Hz); there are $\approx$ 5 ms between machine pulses and the particles are highly collimated into jets, so that high hit densities and pulse pair resolution are important issues. At the τ-charm factory, on the other hand, the trigger rate is fast (up to 1 KHz); there are $\approx$ 50 ns between machine pulses, the typical particle densities are low, and there are only large radius liquid rings so that the number of hits per box will usually be small.

These differences in machine environment lead to several modifications in the electronics. Conceptually, the front-end (preamp) electronics can be just like the SLD CRID (with a different shaping time) but a different readout is required. Full wave form digitization (as in the SLD) is possible, but would be very expensive at these data rates and probably unnecessary. Simple considerations of hit densities expected at the τ-charm factory suggest that four hits per wire should be sufficient. At these hit densities, it is probably much cheaper to read out each wire end by a combination TDC/ADC. A four hit version is indicated schematically in Fig. 3(a). The TDC portion is quite straightforward. There are a variety of ways one might implement the ADC. For example, it could use a simple modification of the SLD CDU [4] module as shown in Figs. 3(b) and 3(c). This is a simple analog storage device with parallel-in, serial-out architecture which has four cells per channel. The exact level of multiplexing into the ADC depends on the readout time desired and on the ADC digitizing speed. In particular, with the 32 preamp multiplexing shown in Fig. 3(c), an ADC with 1.5 μs digitizing speed leads to 20% deadtime at the maximum projected 1 KHz trigger rate.

7. Performance

The particle separation capabilities of the CRID depend primarily on the precision with which the Čerenkov angle is measured, which in turn, depends on the angular precision of each photoelectron measurement and the number of photoelectrons detected. A detailed discussion of the various sources of measurement error and photoelectron production rates are given in Refs. [4 and 11]. For the configuration chosen here, the important contributions to the total error are: (a) geometrical error, which is dominated by the depth of the radiator and the drift space; (b) detector measurement error, which includes diffusion, measurement granularity, and non-uniformities in electron drift in the detector; (c) multiple scattering error in projecting the track measured in the CDC out to the CRID; (d) momentum smearing error due to the bending of the particle in the radiator; and (e) chromatic

aberration error in the radiating liquid. The largest single contribution ($\sim$ 7.3 mr per photoelectron) generally comes from the geometrical term. Typically, the combined contribution from all other terms is about the same size. The size of the geometrical term can only be reduced either by making the radiator thinner, which loses photoelectrons or by making the drift space longer, which makes the overall counter thicker.

The particle separation capabilities of the CRID are shown in Fig. 4. The Monte Carlo particles for results shown here entered the radiator at a polar angle of 64° relative to the beam line, so that these plots include the typical loss of photons due to total internal reflection that occurs when the particles enter the radiator at oblique angles. The vertical scales give the separation between different kinds of particles in "standard deviations (σ)." It is "saturated" at 10σ, since the "Gaussian" separation probabilities estimated here will surely be unreliable for very large estimated separations. The hadronic separations are generally excellent, exceeding 10σ from near threshold up to the highest energies to be seen at the τ-charm factory. The CRID also provides excellent low momentum lepton identification which complements the calorimetry and muon tracking chambers very well. At the 3σ level, e/π separation is achieved up to 1.2 GeV/c, and μ/π separation is achieved up to 0.8 GeV/c. There are regions at the lowest momenta where both particles are below threshold. This is a significant effect only for the K/p case. K threshold in the liquid is at 620 MeV/c. The K/p separation, extends down to $\approx$ 480 MeV/c using radiation from the quartz. For lower momentum, the number of photons produced by the kaon particle becomes too small for reliable separation and, in any case, below 430 MeV/c neither particle emits any photons. However, in cases where particles are too slow to be separated by the Čerenkov it should be very simple to obtain dE/dx separation since one or both particles are far into the $1/\beta^2$ region, where even very modest amplitude information on energy loss will provide excellent separation. There is also a low momentum cutoff due to particle curvature in the magnetic field which depends on the CRID radius, the magnetic field and the polar angle of the particle. For example, a device at 60 cm radius in a

10 KG field is unable to identify a particle traveling perpendicular to the magnetic field below $\sim$ 130 MeV/c. Again, this "hole" in the CRID coverage can be filled with very modest dE/dx information from the CDC in the $1/\beta^2$ region.

8. Summary

The CRID technology described above meets the requirements for particle ID at a τ-charm factory very well indeed. In addition to providing superior $\pi/K/p$ separation, it also fills in the lepton ID holes which are left by the calorimetry and muon tracking techniques. However, the "costs" associated with the technology are substantial. The device is expensive to build; takes 20 cm of space inside the detector volume, which makes the calorimetry more expensive; and adds roughly 20% of a radiation length of material in front of the calorimetry. Whether these costs are justifiable depends on the details of the physics that the detector will address. In particular, the low momentum lepton identification appears to be very powerful. In any case, it seems desirable that a CRID device designed for a general purpose detector be capable of being removed for those experiments where low mass before the electromagnetic calorimetry is essential.

I would like to thank members of the SLD CRID group, with special thanks to Steve Yellin, Gerard Oxoby, and David Leith for stimulating discussions and for their help in preparing material for this talk.

REFERENCES

1. J. Vavra, Proceedings of this Workshop.
2. R. Stroynowski, Proceedings of this Workshop.
3. J. Seguinot and T. Ypsilantis, Nucl. Instr. and Meth. **142** (1977) 377.
4. SLD Collaboration, SLD Design Report, SLAC–Report–273 (1984).
5. CERN/LEPC/83-3 (1983), CERN/LEPC/P2 (1983).
6. CERN/LEPC/84-15 (1984).
7. V. Ashford et al., Proc. of the XXIII International Conf. on High Energy Physics (1986) 1470.
8. R. Arnold et al., Nucl. Instr. and Meth. **A270** (1988) 255.
9. R. Arnold et al., CERN-EP/87-186 (1987); E. Chesi et al., talk presented at the International Wire Chamber Conf., Vienna, Austria (Feb. 1989).
10. J. Kirkby, Proceedings of this Workshop.
11. T. Ypsilantis, Phys. Scr., **23** (1981) 371.

FIGURE CAPTIONS

1) (a) The CRID principle for a liquid radiator device; (b) size and thickness of a ring image produced at 90° in a liquid radiator; (c) photon detector schematic.

2) Conceptual geometry for a CRID: (a) location in the detector; (b) schematic cross section.

3) Conceptual design for CRID readout: (a) four-hit electronics for each wire end; (b) parallel-in, serial-out analog memory unit (1 of 32 channels); (c) preamp multiplexing scheme.

4) Particle separation capability of the liquid CRID system at 64°. The curves are saturated at 10σ (see text). In the dotted regions of the curves, only the lighter particle emits light in the liquid. There are thresholds shown at low momentum below which the lighter particle emits too few photons in either quartz or liquid to be reliably separated (see text). The separation is shown for: (a) e/π; (b) μ/π; (c) π/K; and (d) K/p.

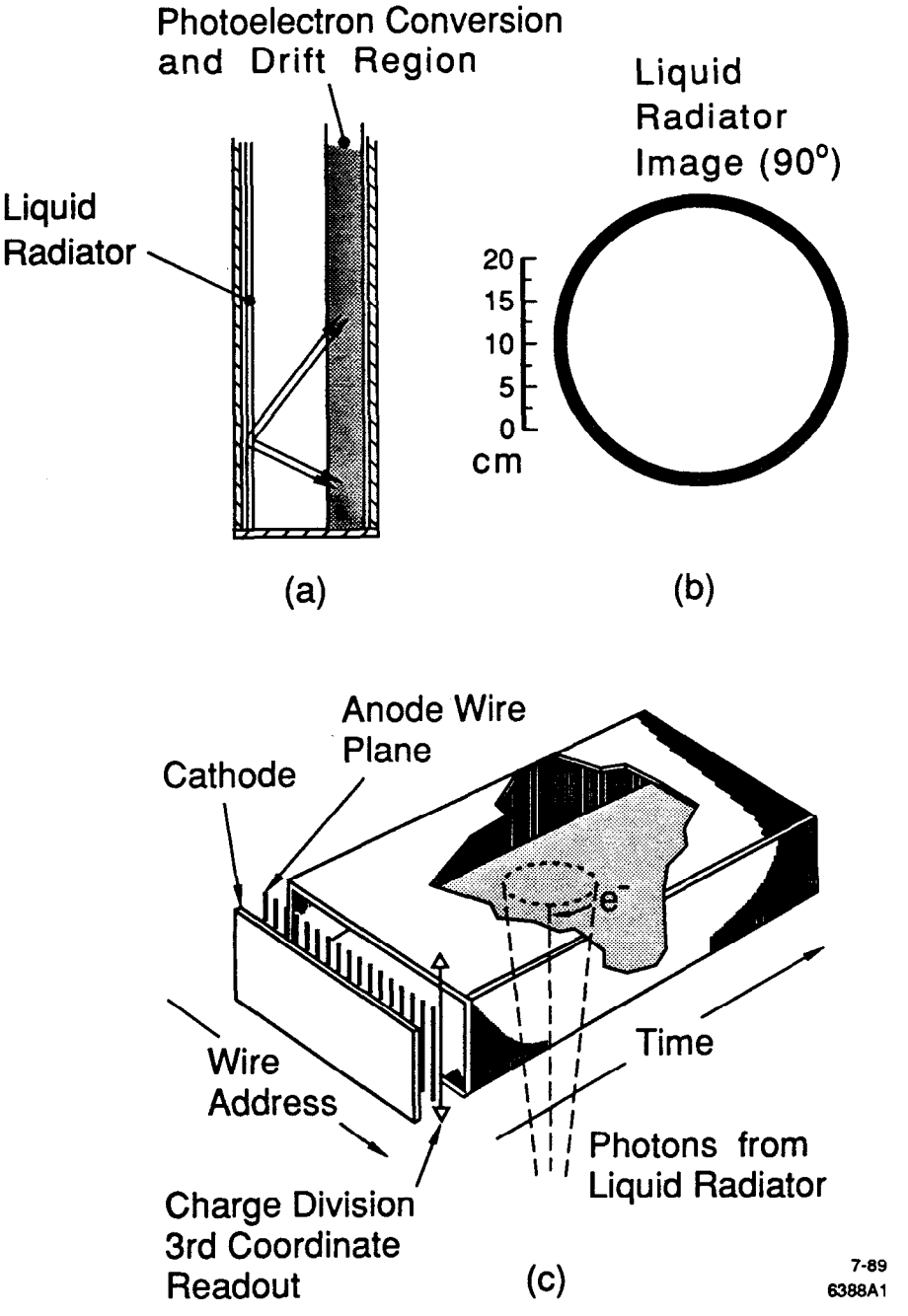
Photoelectron Conversion
and Drift Region
Liquid
Radiator
Liquid
Radiator
Image (90°)
20
15
10
5
0
cm
(a)
(b)
Anode Wire
Plane
Cathode
e⁻
Time
Wire
Address
Photons from
Liquid Radiator
Charge Division
3rd Coordinate
Readout
(c)
7-89
6388A1

Figure 1

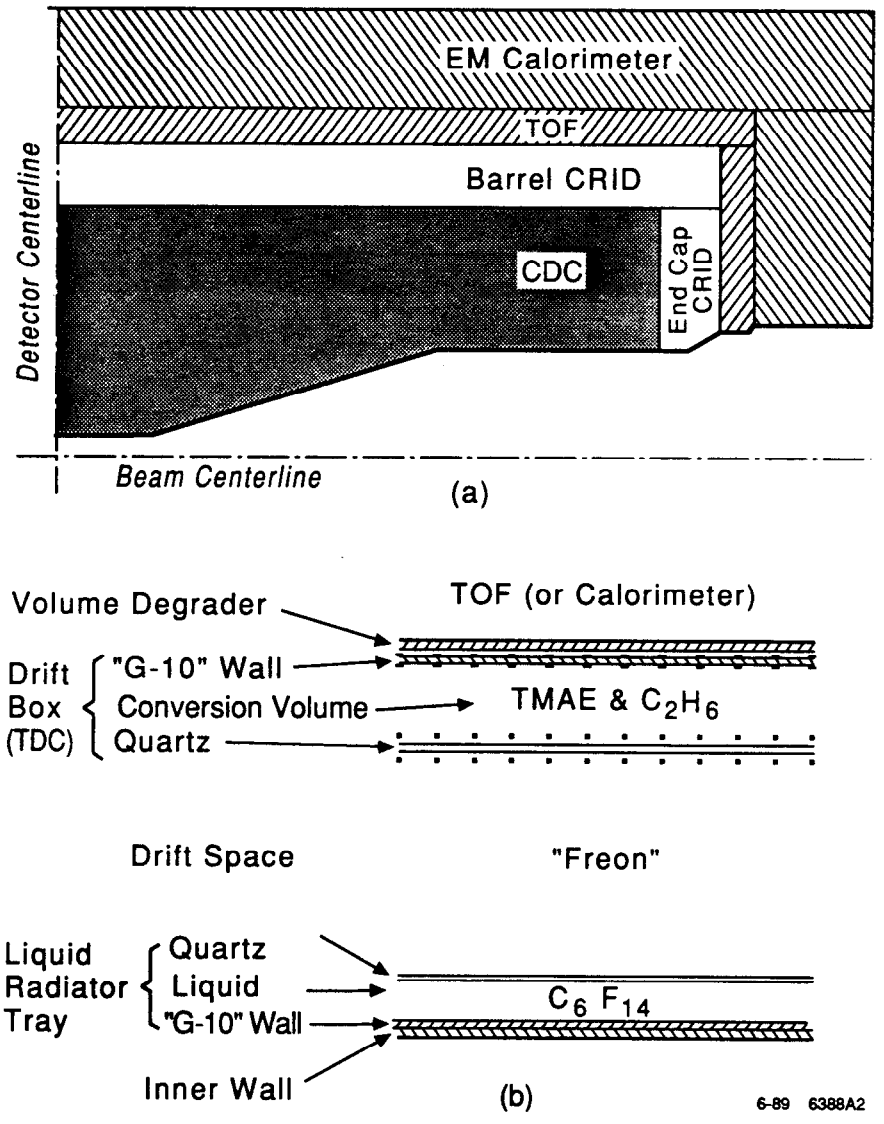
EM Calorimeter
TOF
Barrel CRID
CDC
End Cap CRID
Detector Centerline
Beam Centerline
(a)
Volume Degrader
TOF (or Calorimeter)
Drift Box (TDC)
"G-10" Wall
Conversion Volume
Quartz
TMAE & C_2H_6
Drift Space
"Freon"
Liquid Radiator Tray
Quartz
Liquid
"G-10" Wall
Inner Wall
C_6F_{14}
(b)
6-89 6388A2

Figure 2

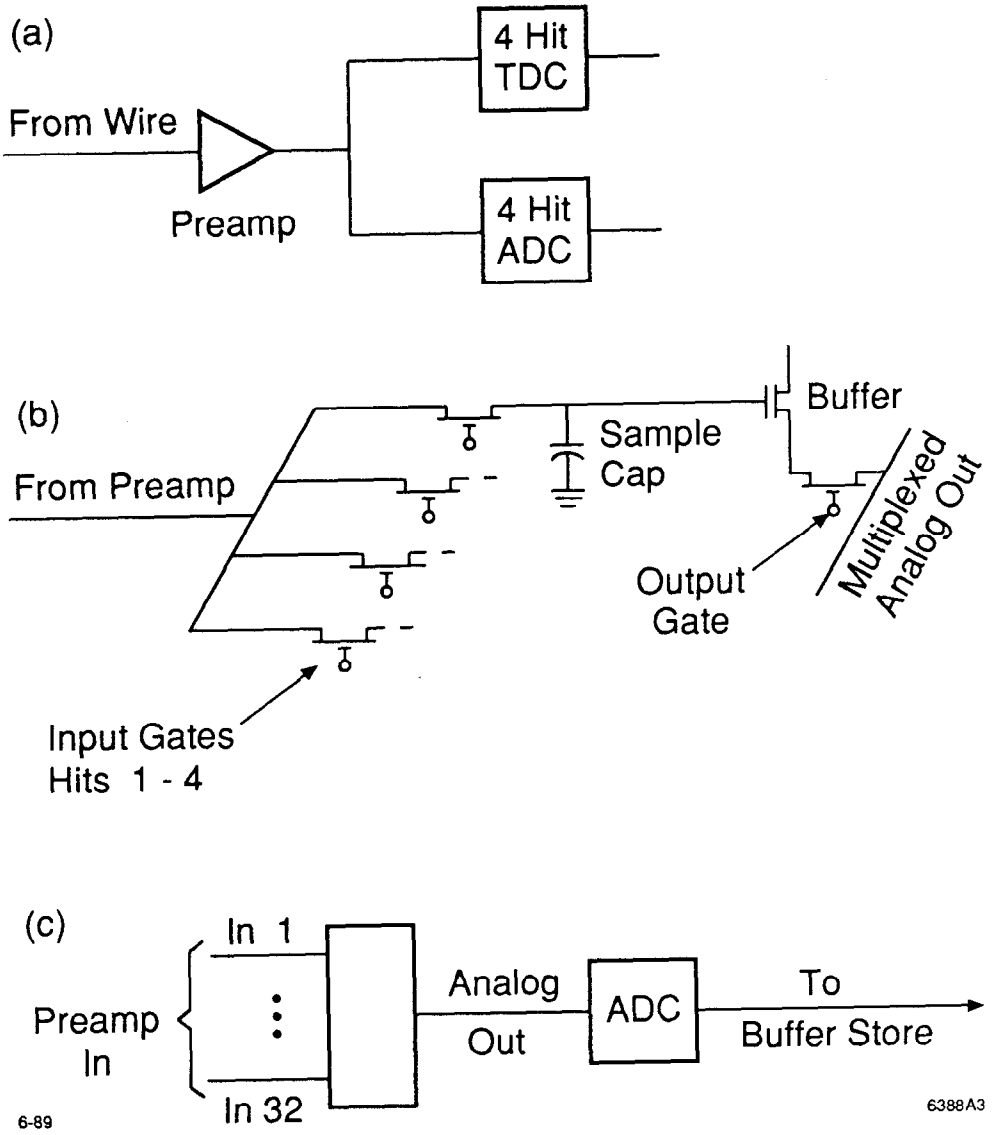
(a)
From Wire
Preamp
4 Hit
TDC
4 Hit
ADC
(b)
From Preamp
Sample
Cap
Buffer
Multiplexed
Analog Out
Output
Gate
Input Gates
Hits 1 - 4
(c)
Preamp
In
In 1
In 32
Analog
Out
ADC
To
Buffer Store
6-89
6388A3

Figure 3

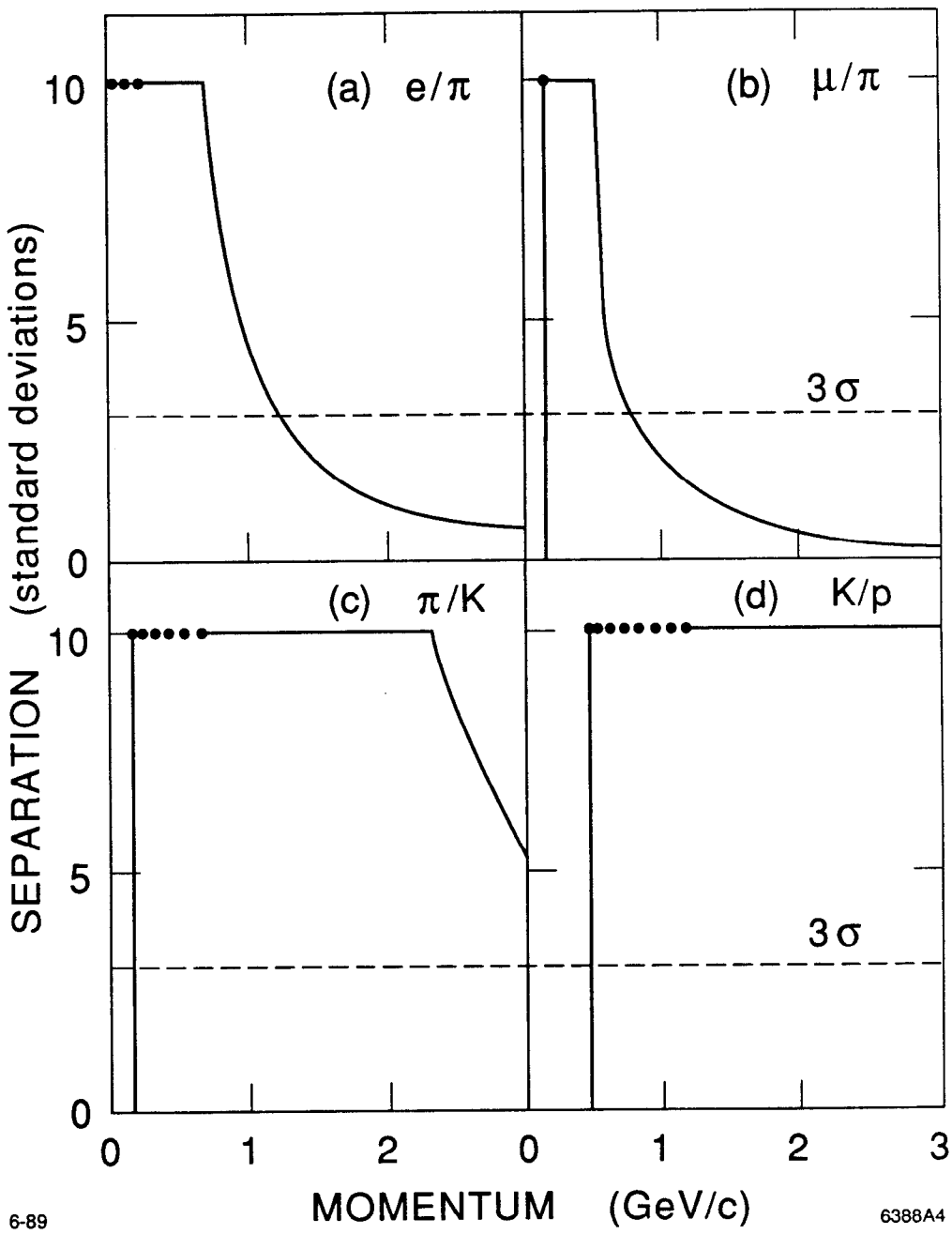
(a) e/π
(b) μ/π
(c) π/K
(d) K/p
3σ
3σ
10
5
0
10
5
0
SEPARATION (standard deviations)
0
1
2
0
1
2
3
MOMENTUM (GeV/c)
6-89
6388A4

Figure 4